Computer Simulation Study of Patterns of Copper and Silver Dendrites Grown from Aqueous Solution in High Magnetic Field

Wenyong Duan, Masao Fujiwara, and Yoshifumi Tanimoto*

Graduate School of Science, Hiroshima University, Kagamiyama, Higashi-Hiroshima 739-8526

(Received April 7, 2000)

The magnetic field effects (MFEs) on the patterns and yields of silver and copper dendrites generated from Cu^{2+}/Zn and Ag^{+}/Cu liquid–solid redox reactions are simulated with the aid of a biased random walk model. In the present model, multi-particles are generated to represent metal ions, and their trajectories walk randomly with superimposed drifts. Comparing the simulation patterns and yields with the experimental ones, it is confirmed that the convection of solution induced by the magnetic force is responsible for the observed MFEs on the dendrites in a high magnetic field gradient (ca. 400 $T^2\,m^{-1}$).

Studies of effects of high magnetic field (> 2 T) on chemical, physical, and biological processes are now important.[1] This is partly because high magnetic fields have potential for producing materials with improved quality. We have researched the effects of high magnetic field ($\leqq$ 13 T) on chemical,[2,3] physical[4] and biological systems.[5] In the course of these studies, it has been found that a high magnetic field gradient drastically affects patterns of silver and copper dendrites generated by the liquid-solid redox reactions.[3a,3b,3d] It is proposed that the magnetic force induced by a high magnetic field gradient influences the dendritic patterns.

Diffusion-limited aggregation (DLA) has stimulated intensive interest over the last two decades. Many experiments and computer simulation studies have been focused on this subject.[6—11] Witten and Sander[7b] introduced the DLA model to produce the random fractal pattern in irreversible aggregation, and simulated the irregular and self-similar patterns. Meakin[8b] studied the influence of unidirectional particle drifts of the DLA pattern with a Monte Carlo method and found that the resulting clusters have uniform structure on all but the shortest length scales if particle drift effects are dominant. Nagatani and Sagues[10b] studied the morphological evolution of DLA deposited on a line by changing the direction of the hydrodynamic flow. In their model, the morphology was greatly influenced by the direction and strength of flow.

In order to verify the mechanism of magnetic field effects (MFEs) on the silver dendrite grown from aqueous solution, we have simulated its patterns by an one-particle random walk model and have suggested that convection of solution induced by a magnetic field gradient is responsible for the observed effects.[3c] We attempted to simulate patterns of copper dendrite grown from aqueous solution using the same model, as it is urgent to elucidate the mechanism of MFEs on copper dendrite. The patterns of copper dendrite are very different from those of silver dendrite and it was found that the model used was not suitable for the simulation of the copper dendrite, since it could not reproduce the patterns at zero field. This is partly because it is too simple to simulate dendritic patterns of different morphology.

In this paper, a biased multi-particle random walk model with improved flexibility is applied to simulate patterns of both copper and silver dendrites in order to clarify the mechanism of the MFEs. Patterns of dendrites in the absence and presence of a magnetic field gradient are well simulated with the aid of this new and simple model. It is confirmed that the convection of solution induced by the magnetic force contributes chiefly to the dendritic patterns and yields in a magnetic field gradient.

Model for Computer Simulation

Experimental Results. For the sake of consideration of a model for computer simulation, experimental results for the present liquid-solid redox reactions are given briefly.[3a,3b,3d] The copper and silver dendrites are formed by the simple liquid-solid redox reactions,

$$Zn + Cu^{2+} \rightarrow Zn^{2+} + Cu \downarrow \quad (1)$$

$$Cu + 2Ag^{+} \rightarrow Cu^{2+} + 2Ag \downarrow \quad (2)$$

under the experimental condition shown in Fig. 1. In reaction (1), a zinc wire is placed on a strip of chromatography paper wet with 0.5 mol dm^{-3} $CuCl_2$ aqueous solution in the absence and presence of a magnetic field gradient shown in Fig. 1, whereas in reaction (2) a copper wire is placed on a strip of chromatography paper wet with 0.5 mol dm^{-3} $AgNO_3$ aqueous solution.

Figure 2 shows the patterns of copper dendrite in the absence (a) and presence (b) of a magnetic field of B_{max} = 8 T. B_{max} is the maximum magnetic field at the center of a bore tube and is used as a representative of the magnetic field gradient depicted in Fig. 1. Figure 3 shows the patterns of silver

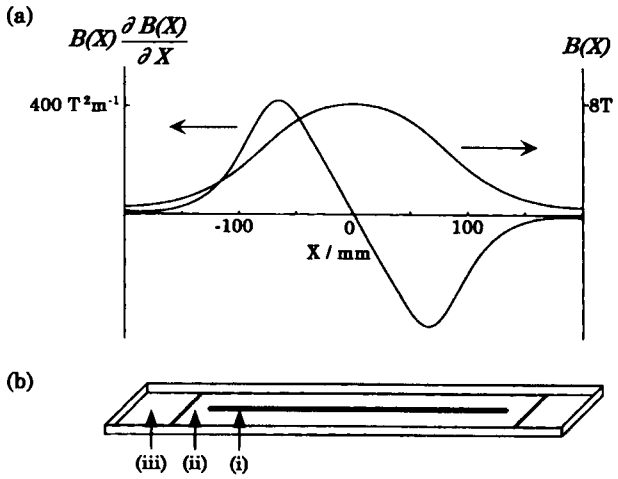

Fig. 1. (a) The distribution of the magnetic field $B(X)$ and the product of the magnetic field and the magnetic field gradient $B(X)\partial B(X)/\partial(X)$, X being the distance from the center of the magnetic field. (b) Experimental setup for deposition of metal dendrites. (i) a metal wire ($6\phi \times 250$ mm), (ii) a strip of chromatography paper (300×37 mm), and (iii) a plastic vessel (40 mm × 380 mm × 10 mm).

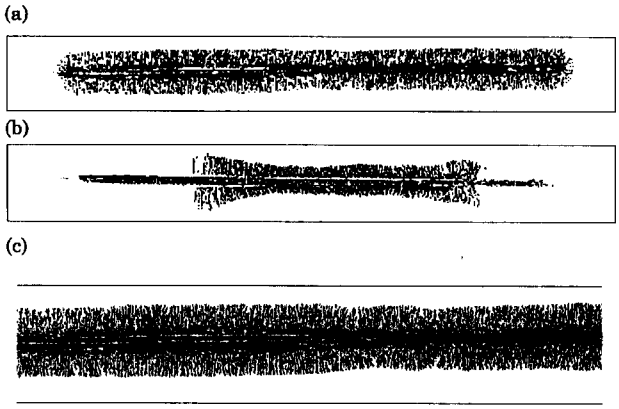

Fig. 2. Patterns of copper dendrite generated from the Cu^{2+}/Zn redox reaction obtained experimentally. (a) B_{max} = 0 T. (b) B_{max} = 8 T. (c) Enlarged pattern at B_{max} = 0 T.

dendrite in the absence (a) and presence (b) of the magnetic field. The patterns of copper dendrite are very different from those of silver metal at zero field, as shown in Figs. 2(c) and 3(c). The copper dendrite grows almost perpendicularly to the wire, whereas that of silver grows almost randomly into four directions. Although we do not know the reason for this difference, a plausible explanation may be that the crystal habits are different in two metals. The dendritic patterns of copper and silver change very significantly by the application of the magnetic field. In the case of copper dendrite in a magnetic field (Fig. 2(b)), it grows heavily in the center part of the paper, whereas it is rather sparse at the two ends of the wire. In good contrast with reaction (1), silver dendrite grows mainly at the two ends of the wire. The drastic changes in dendritic patterns are mainly attributed to the magnetic field-induced convection of the solution which is held in the thin layer between the chromatography paper and the bottom of the vessel.[3d]

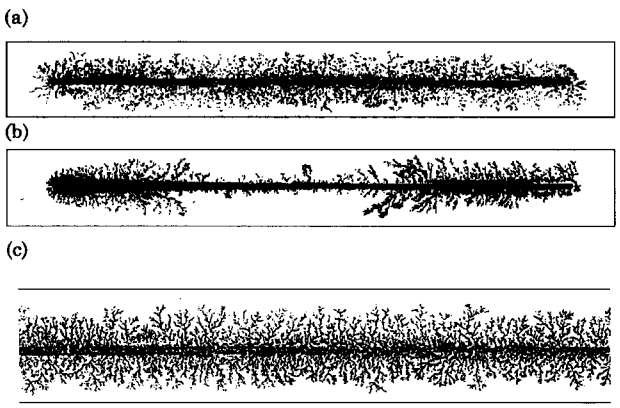

Fig. 3. Patterns of silver dendrite generated from the Ag^{+}/Cu redox reaction obtained experimentally. (a) B_{max} = 0 T. (b) B_{max} = 8 T. (c) Enlarged pattern at B_{max} = 0 T.

Simulation Model. In order to simulate the experimental results shown in Figs. 2 and 3, the following random walk model is applied. Simple rectangle lattices (601×75) are used to represent a strip of chromatography paper, as shown in Fig. 4. The origin of the x and y coordinates in the lattice is taken to be at the center of the two-dimensional lattices. Five rows, i.e., [(−245, y) to (245, y), $y = 0, \pm1, \pm2$], are used as the occupied lattices that represent the metal wire. A total number of N_T particles which represent metal ions are randomly generated on the lattices. Every particle has equal "move probability, P_0", to move in four directions. A random number, r, in the range of 0—1 is generated to decide in which direction a particle should move. If r is in a range of the move probability of any direction, then it moves by one lattice unit in that direction. For example, if $P_0 = 0.25$, a particle moves to x ($0 \leqq r < 0.25$), $-x$ ($0.25 \leqq r < 0.5$), y ($0.5 \leqq r < 0.75$), and $-y$ direction ($0.75 \leqq r \leqq 1.0$) depending on r. If there is another particle already occupying that site, the particle does not move but remains at its old site. When a new site of a particle is out of the rectangle lattice, it remains at its old site.

When a particle reaches a site that is the most adjacent to the metal wire or the growing dendrite, whether it sticks to the dendrite or not as a metal particle is decided using "stick probability, S". Stick probabilities, S_x, S_y and S_{xy}, for example, are the ones in different directions as shown in Fig. 4. The site occupied by the particle is surrounded by 8 neighboring sites with eight stick probabilities, the origin of their directions being taken at the site occupied by the particle. If any of these neighboring sites are occupied by the dendrite, the site of the highest stick probability is selected from the unoccupied sites. Then, a random number, r, is generated. When r is smaller than or equal to the stick probability of that site, the particle sticks to that site; otherwise it remains at that site. In the following, $S_x = S_{-x}$, $S_y = S_{-y}$, and $S_{xy} = S_{-xy} = S_{x-y} = S_{-x-y}$ are assumed.

Furthermore, metal particles must form a cluster in order to be recognized as a part of metal dendrite. For this purpose, "clustering number, N_c", is introduced. When it is occupied by N_c particles, a lattice is incorporated into a part of the

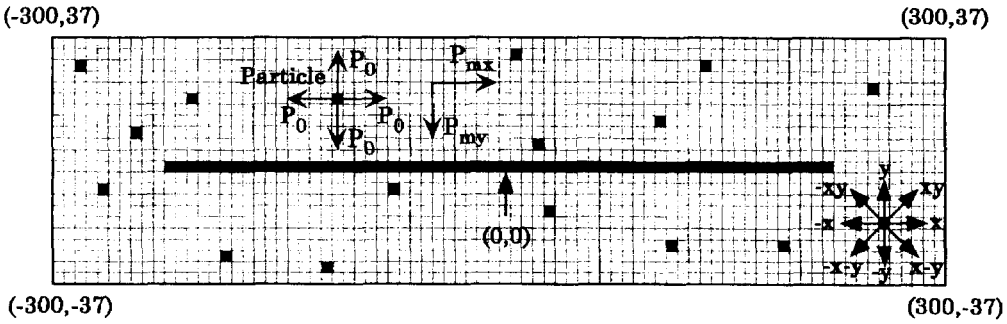

Fig. 4. The model used for computer simulation of dendritic patterns in a magnetic field gradient.

dendrite.

If the solution that contains particles flows in one direction, "drift probability, P_m" is added to the move probabilities of particles in that direction, and the particles have more probability to move in that direction. Move probabilities of particles are varied to adjust the direction and the strength of the drift. The trajectories of particles are random walks on short length scales, whereas on long length scales they will show some effects of the drift. Detailed treatment of P_m is given below.

The simulation was carried out for N_T particles. The simulation is ended when a certain number of particles, N_D, are deposited or when steps of random walk become a certain number of steps, N_S, which represents the reaction time. The calculation was carried out using a personal computer (NEC, PC98-21).

Result and Discussion

There are many reports on the DLA models. A variety of effects are introduced in them by taking account of particle drift,[8b,10b] finite density of aggregation particles,[8c,11a] or stick probability.[11b] In the present model, the following are introduced in the calculation: (1) In order to simulate the dendritic patterns realistically, a random walk of multi-particles model is applied as, in the experimental conditions, about 10^{22} particles of ions and water molecules move in the thin layer of 37 mm×300 mm and about 25% of metal ions are reduced into metals in the reaction. (2) Dendrites are generated starting from the multiple seeds forming rows, though they are usually grown starting from a single seed. (3) In order to simulate patterns with different morphology at zero field, stick probabilities are introduced. (4) In order to change density of dendrites, the clustering number is introduced. Motions of Cu^{2+} or Ag^+ ions are only treated in a representative way, though in actual experimental conditions a solution composed of cations, anions, and water molecules moves by convection.

After simulating the patterns at zero field, we simulate patterns in the magnetic field by introducing drift probability which is related to the magnetic field-induced convection. The simulation is carried out for $N_T = 20,000$. This means that about 44% of lattices are occupied initially by particles.

1. Simulation Patterns at Zero Field. Influence of Clustering Number and Stick Probability. Before simulating observed patterns of dendrites, let's examine the influence of clustering number, N_c and stick probability, S, on the patterns of dendrites. Figure 5 shows the influence of N_c. When $N_c = 1$, the density of dendrite is very high. When $N_c = 3$, the dendrite grows sparsely. By introducing N_c, the density of dendrite deposited is controlled. In the following simulation, N_c is fixed at 2.

In order to reproduce different patterns of dendrites, "stick probability, S" is introduced in the present model. Figure 6 shows the influence of S on the patterns of dendrite. When stick probabilities are the same in all directions, i.e., $S_x = S_y = S_{xy} = 1$, the dendrite grows with the same ratio in all directions and its branches spread widely (Fig. 6(a)).

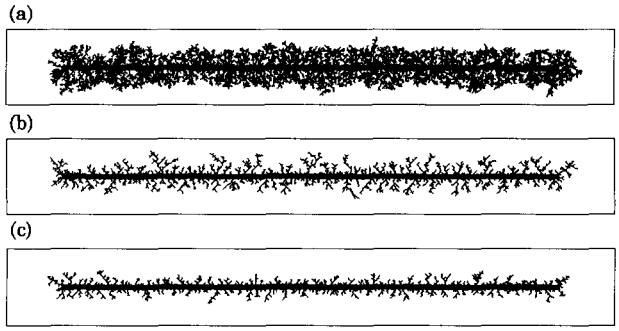

Fig. 5. Influence of clustering number, N_c, on the simulated pattern. $N_T = 20,000$, $N_D = 8,000$, $P_0 = 0.25$, $S_x = S_y = S_{xy} = 1$. (a) $N_c = 1$. (b) $N_c = 2$. (c) $N_c = 3$.

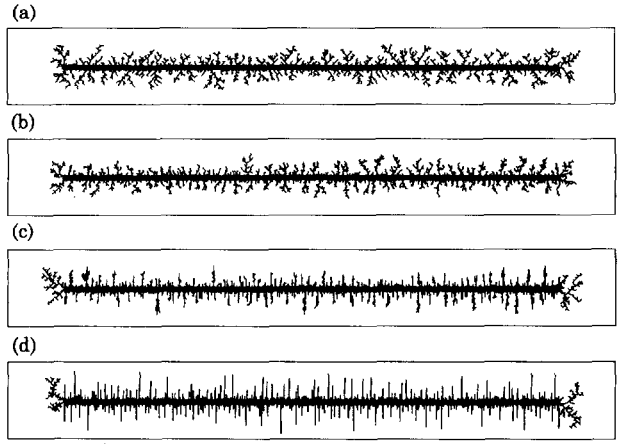

Fig. 6. Influence of stick probability, S, on the simulated pattern. $N_T = 20,000$, $N_D = 8,000$, $N_c = 2$, $P_0 = 0.25$. (a) $S_x = 1$, $S_y = 1$, $S_{xy} = 1$. (b) $S_x = 0.5$, $S_y = 1$, $S_{xy} = 0.5$. (c) $S_x = 0.2$, $S_y = 1$, $S_{xy} = 0.2$. (d) $S_x = 0$, $S_y = 1$, $S_{xy} = 0$.

When the values of S_x and S_{xy} are decreased, the dendrite grows more slowly in x and xy directions than in y direction (Fig. 6(b,c)). When $S_x = S_{xy} = 0$, and $S_y = 1$, the dendrite can only grow in y direction, and the branches become almost perpendicular to the wire (Fig. 6(d)). The patterns shown in Figs. 6(a) and 6(b) are similar to the dendritic patterns of silver at zero field (Fig. 3(c)), whereas those shown in (c) and (d) are similar to those of copper at zero field (Fig. 2(c)). By introducing anisotropic stick probabilities in simulation, we can generate dendrites with different morphology at zero field.

In the following, the simulation pattern in Fig. 6(c) is taken as the representative of copper dendrite at zero field, whereas that in Fig. 6(a) is taken as that of silver dendrite. The parameters used there are fixed and a new parameter, P_m, is added in simulation of patterns of respective dendrites in a magnetic field gradient.

2. Dendritic Patterns in a Magnetic Field Gradient. When a magnetic field is applied, the deposition patterns change drastically. The magnetic field gradient induces a magnetic force, which is given by

$$F_{mag}(X) = (\chi/\mu_0)B(X)\partial B(X)/\partial X \quad (3)$$

where χ is the magnetic susceptibility, μ_0 is the magnetic permeability, $B(X)$ is the magnetic field intensity at the position X, X being the distance from the position of the maximum magnetic field. Ag^+ ion, Zn^{2+} ion, their counter ions and water are all diamagnetic. The effect of the magnetic force on diamagnetic ions can be negligible because of their small χ values. It is considered that paramagnetic Cu^{2+} ion is affected by the magnetic force. This is because the absolute value $|\chi|$ of Cu^{2+} ion is about two orders of magnitude larger than those of diamagnetic species. It is also known that the redox reactions in which paramagnetic ions are involved are only affected by the external magnetic field.[3b]

In order to simulate patterns of dendrites in a magnetic field gradient, the drift of particles by the magnetic force is introduced in the calculations.

Copper Dendrite. The copper dendrite is formed by reaction (1). At zero field the copper dendrite grows almost perpendicularly to the wire. This pattern can be reproduced by the parameters applied for the simulation of the one shown in Fig. 6(c). Then patterns of copper dendrite in a magnetic field gradient are simulated for two cases, Case A and Case B, by introducing a drift probability P_m.

In Case A, only Cu^{2+} ions are considered to move to the higher field by the magnetic attractive force as depicted in Fig. 7(a). Then the drift probability $P_{mx}(x)$, which represents the drift probability in x direction at a column [x] of lattices, is added in the directions to the higher field (x or $-x$) so that the particles have a higher probability to move in that direction. It is assumed that $P_{mx}(x)$ is proportional to the magnetic force $F_{mag}(X)$ (Eq. 3) and that the maximum value of $P_{mx}(x)$ is P_m, as depicted in Fig. 8. The sum of $P_{mx}(x)$ and $4P_0$ is normalized to 1. For example, the values of $P_{mx}(x)$ at the column A [0] which corresponds to the center of the wire, the column B [130] where the F_{mag} is the maximum value and the column C [245] which corresponds to the end of the wire in the first quadrant in Fig. 7(a) are: $P_{mx}(0) = 0$; $P_{mx}(130) = P_m$; $P_{mx}(245) = 0.218P_m$. The drift probability $P_{mx}(x)$ increases from 0 at the column A to the maximum value (P_m) at the column B, and then decreases to $0.218P_m$ at the column C.

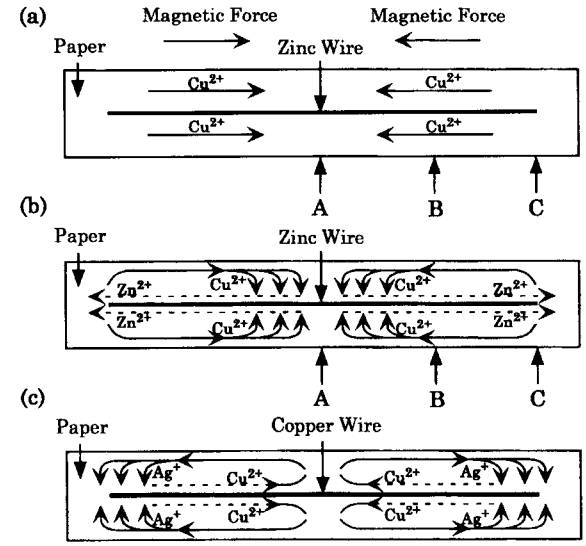

Fig. 7. Directions of flow of particles assumed in simulation of copper and silver dendrite patterns. (a) Copper dendrite (Case A). (b) Copper dendrite (Case B). (c) Silver dendrite. A, B, and C in the figure indicate locations of columns of [0], [130], and [245], respectively.

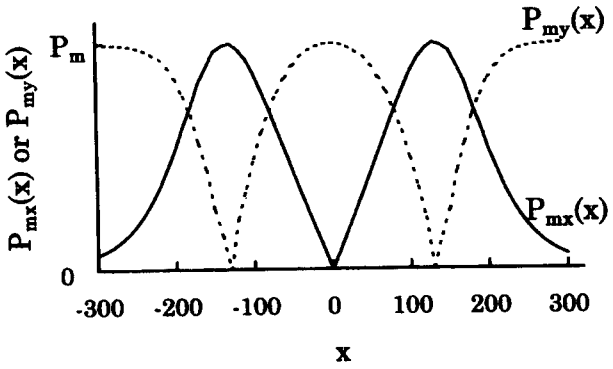

Fig. 8. $P_{mx}(x)$ and $P_{my}(x)$ used in simulation.

Figure 9 shows the simulation patterns of copper dendrite in a magnetic field. Figure 9(a) is the pattern at zero field and (b) is that in Case A with $P_m = 0.2$. This simulation pattern is similar to the one shown in Fig. 9(a) and is very different from the observed one shown in Fig. 2(b). It is obvious that this model, where only the drift of Cu^{2+} ion to the center part of the paper is considered, can not reproduce the observed pattern at all.

It is experimentally known that, after the reaction, Zn^{2+} ions remain mainly in the neighborhood of the two ends of a zinc wire, whereas copper dendrite grows mainly in the center part of the paper. This observation can be explained only by the convection of solution which is induced by the mag-

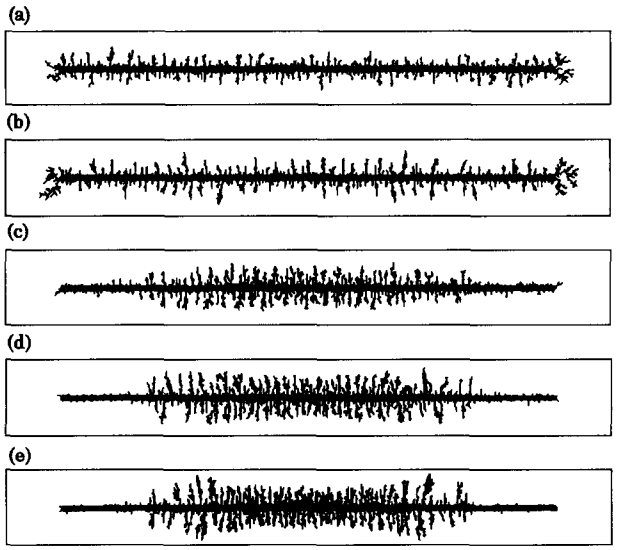

Fig. 9. Influence of drift probability, P_m, on simulated patterns of copper dendrite. $N_T = 20,000$, $N_s = 3,000,000$, $N_c = 2$, $S_x = 0.2$, $S_y = 1$, $S_{xy} = 0.2$. (a) $P_m = 0$. (b) Case A (flow directions of particles depicted in Fig. 7(a) are assumed). $P_m = 0.2$. (c) Case B (flow directions of particles depicted in Fig. 7(b) are assumed). $P_m = 0.1$. (d) Case B. $P_m = 0.2$. (e) Case B. $P_m = 0.3$.

netic force. Convection means the displacement of solution as a whole and does not mean the displacement of solutes in it. Since, in Case A, only motion of Cu^{2+} ions is considered, this model corresponds to the magnetic field-induced diffusion of Cu^{2+} ions and is concluded to be inadequate to represent the pattern of copper dendrite in a magnetic field.

In a previous paper,[3d] it is suggested that not a solution adsorbed by the chromatography paper but a mobile solution (0.6 ml) in the thin layer between a chromatography paper and the bottom of a plastic vessel undergoes convection. In convection of solution, if a part of solution in the layer moves to a certain direction, there must exist a counter flow at another part of the solution. A mobile solution must flow continuously within the area covered by the paper.

In Case B, it is assumed that the Cu^{2+} ions move, as a result of convection of solution, in the directions depicted in Fig. 7(b). Under the experimental condition shown in Fig. 1, the solution apart from the zinc wire is rich in paramagnetic Cu^{2+} ions, whereas that in the neighborhood of the wire is poor in Cu^{2+} ions because the redox reaction takes place in the vicinity of the wire. The solution apart from the wire which is rich in Cu^{2+} ions moves to the higher field by the magnetic force. However, at the center of the magnetic field, the magnetic forces from the two sides are compensating each other and the solution can not move further to the same direction. Since the magnetic force on the solution near the wire is weaker than that on the solution apart from the wire, the solution at the center of the magnetic field may turn its direction as shown in Fig. 7(b). As a result, the solution near the wire may be pushed out to the lower field. Since the flow of solution should be continuous, the solution near the two edges may also turn its direction as depicted in the figure. It is said that, in the case of copper dendrite, a magnetic field induces convection by affecting the paramagnetic *reactant* in reaction (1).

Based on the argument briefly mentioned above, the directions of convection depicted in Fig. 7(b) are assumed in Case B. In the calculation, it is assumed that the drift probability is a function of x, though it would be a function of x and y in the 2-dimensional lattices. This assumption is adopted to simplify the calculation procedure. The drift probability is divided into two components, $P_{mx}(x)$ and $P_{my}(x)$, which represent the drift probabilities in x and y directions at a column [x] of lattices, where $P_m^2 = P_{mx}(x)^2 + P_{my}(x)^2$ and the sum of P_m and $4P_0$ is normalized to 1. $P_{mx}(x)$ is assumed to be proportional to $F_{mag}(X)$ and, therefore, is identical with the value in Case A. $P_{my}(x)$ is obtained from the equation, $P_{my}(x)^2 = P_m^2 - P_{mx}(x)^2$, for a given value of P_m. The values of $P_{mx}(x)$ and $P_{my}(x)$ are depicted in Fig. 8. For example, the values of $P_{mx}(x)$ and $P_{my}(x)$ at the columns A [0], B [130] and C [245] in the first quadrant in Fig. 7(b) are: $P_{mx}(0) = 0$ and $P_{my}(0) = P_m$; $P_{mx}(130) = P_m$ and $P_{my}(130) = 0$; $P_{mx}(245) = 0.218P_m$ and $P_{my}(245) = 0.976P_m$. The move probability $P_{mx}(x)$ increases from 0 at the column A to the maximum value (P_m) at the column B, and then decreases to $0.218P_m$ at the column C. On the other hand, the probability $P_{my}(x)$ decreases gradually from P_m at the column A to 0 at the column B and then increases gradually up to $0.976P_m$ at the column C. Particles move to the wire (i.e., y or $-y$ direction) in addition to the movement to the higher field (i.e., x or $-x$ direction). Here convection of solution in the lattices where dendrites are already deposited is not taken into account by the calculation.

Figure 9(a,c—e) shows the influence of P_m on the patterns of dendrite in Case B. When P_m is increased from 0 to 0.3, most particles move to the center part of the paper and the dendrite grows thickly there. Only very few particles deposit at the two ends of the zinc wire. The simulation patterns (d) and (e) are similar to the experimental one in the magnetic field (Fig. 2(b)), indicating that the experimentally observed patterns of copper dendrite are formed by the influence of convection of solution shown in Fig. 7(b).

The assumption that P_{mx} and P_{my} are dependent only on x does not represent the counter flow near the wire, as the solution near the wire is expected to move to the lower magnetic field. This does not influence significantly the patterns of dendrite as shown in Fig. 8(d, e). At a short time after the reaction starts, this might affect the patterns of dendrite. As the reaction proceeds, however, the Cu^{2+} ions in the neighborhood of the wire disappear rapidly and, therefore, motion of the ions in the neighborhood of the wire may not affect patterns of dendrite deposited apart from the wire, since the counter flow takes place where Cu^{2+} ions are already reacted. Similarly, neglect of convection of solution in the lattices where dendrites are already deposited does not influence significantly the patterns of dendrite.

Silver Dendrite. The silver dendrite grows by reaction (2). At zero field, silver ions move toward the copper wire by diffusion and deposit around it as shown in Fig. 3(a). This

pattern can be reproduced by the parameters applied for the simulation at zero field shown in Fig. 6(a). In this reaction, it is considered that a magnetic force affects paramagnetic products, Cu^{2+} ions, generated by the reaction. The effect of a magnetic field gradient is explained as described below. As the redox reaction proceeds, Cu^{2+} ions are formed near the copper wire. Since Cu^{2+} ions are paramagnetic, the solution near the wire which is rich in Cu^{2+} ions is attracted to the higher field. This induces convection of solution in the thin layer between the chromatography paper and the bottom of the plastic vessel, as depicted in Fig. 7(c). As a result, a counter flow occurs to the lower field in the area apart from the wire, where Ag^+ ion is rich, and silver dendrite grows mainly at the two ends of the copper wire.

Patterns of silver dendrite are simulated analogously by assuming the *counter flow* of Ag^+ ions shown in Fig. 7(c). The values of $P_{mx}(x)$ and $P_{my}(x)$ are the same as those used for copper dendrite deposition in Case B, shown in Fig. 8, except that their directions are opposite.

Figure 10 shows the influence of P_m on the patterns of silver dendrite. Silver dendrite grows preferentially at the two ends of the wire and branches of silver dendrite between the edge and center of the wire bend to the higher field. When P_m is increased from 0 to 0.3 to enhance the effect of the convection, the branches of silver dendrite tilt to the higher magnetic field. The inclined angle is related to P_m, or to the strength of the convection induced by the magnetic force. The area where silver dendrite sparsely deposits increases. The patterns (c) and (d) shown in Fig. 10 resemble well the experimentally obtained one shown in Fig. 3(b). Therefore, the MFE on the patterns of silver dendrite can be explained by the convection of solution depicted in Fig. 10(c).

3. Chemical Yields of Dendrites. It is expected that the magnetic field-induced convection may affect chemical yield of dendrite as well. If the convection assumed in simulating dendritic patterns mentioned above is correct, the MFE on the chemical yield of dendrites should be also reproduced by using the same model.

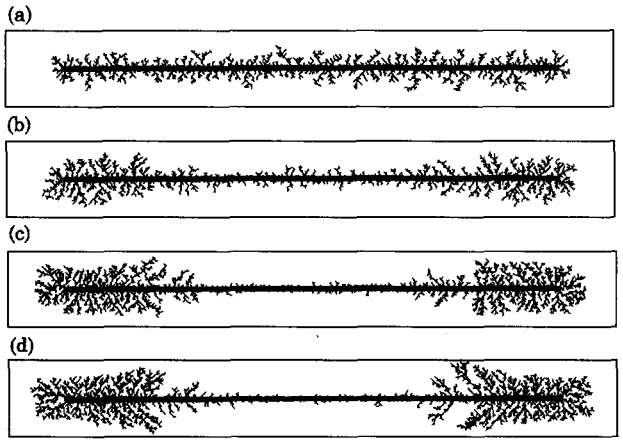

Fig. 10. Influence of drift probability, P_m, on the simulated pattern of silver dendrite. Flow directions of particles depicted in Fig. 7(c) are assumed. $N_T = 20,000$, $N_s = 2,000,000$, $N_c = 2$, $S_x = 1$, $S_y = 1$, $S_{xy} = 1$. (a) $P_m = 0$. (b) $P_m = 0.1$. (c) $P_m = 0.2$. (d) $P_m = 0.3$.

Table 1. Influence of P_m on the Number of Deposited Particles and the Deposition Ratio for Copper Dendrite.

P_m	Number of Deposited Particles	Deposition Ratio
0	7304	1
0.1	8713	1.19
0.2	11048	1.51
0.3	11922	1.63

Parameters used are given in Fig. 9.

Copper dendrite. It is reported that the yield of copper dendrite after one hour reaction is 36±2 mg at zero field, whereas it is 56±12 mg in the presence of a magnetic field gradient ($B_{max} = 8$ T).[3d] The deposition ratio, i.e., the ratio of the yields in the presence and absence of a magnetic field ($B_{max} = 8$ T) is about 1.55.

In our simulation the number of particles deposited within a fixed number of steps, which is equivalent to a fixed reaction time, is counted at several P_m values, other parameters being the same to those used for simulating the pattern at zero field shown in Fig. 9(a). The chemical yields of dendrite in Case B which correspond to the simulation patterns shown in Fig. 9(a,c—e) are listed in Table 1. At zero field, i.e., $P_m = 0$, 7304 particles deposit, and with increasing P_m values from 0 to 0.3 the number of particles increases significantly. The deposition ratio at $P_m = 0.3$ and $P_m = 0$ is 1.63.

The increase in the deposition ratio is in good agreement with the increase in the ratio of copper dendrite in a magnetic field (1.55). It can be said that the convection of the solution induced by the magnetic force contributes chiefly to an increase in the yield of copper dendrite in a high magnetic field gradient.

For the purpose of comparison, the deposition ratio for Case A is calculated. The ratio is 1.11 when $P_m = 0.2$, which corresponds to the pattern shown in Fig. 9(b). It is much smaller than the corresponding value (1.51) calculated for Case B. This small MFE obtained for case A is due to the absence of the probability $P_{my}(x)$. Although a larger MFE on the yield would be achieved by using a larger P_m value, the magnetic force-induced diffusion of copper ions does not seem important. This is because the dendritic pattern shown in Fig. 9(b) is very different from the observed one as discussed above. Furthermore, MFEs on silver deposition can not be explained in terms of the above mechanism. It can be said that the spatial movement of particles is reflected more sensitively in the dendritic pattern than in the chemical yield.

Silver Dendrite. It is reported that the deposition ratio of silver dendrite is 1.45.[3b] This increase in the ratio can also be interpreted by the enhancement of mass transfer of Ag^+ ions, which is induced by the convection of the solution in the magnetic field. Table 2 shows the yields of dendrite which correspond to the deposition patterns shown in Fig. 10(a—d). When P_m increases from 0 to 0.3, the number of the deposited particles increases from 7294 to 11257. The de-

Table 2. Influence of P_m on the Number of Deposited Particles and the Deposition Ratio for Silver Dendrite.

P_m	Number of Deposited Particles	Deposition Ratio
0	7294	1
0.1	7817	1.07
0.2	9747	1.34
0.3	11257	1.54

Parameters used are given in the Fig. 10.

position ratio at $P_m = 0.2$ and $P_m = 0$ is about 1.34. It is in agreement with the increase in the yield of silver dendrite in a magnetic field (1.45). It can be said that the convection of the solution induced by the magnetic force contributes chiefly to the increase in the yield of silver dendrite in a high magnetic field gradient.

Therefore, from computer simulation, the MFE on the yields of both copper and silver dendrite can be also explained by the magnetic field-induced convection of solution, though the magnetic force affects a paramagnetic *reactant* in the former, whereas it affects a paramagnetic *product* in the latter. The most striking feature of the present results is that magnetic field-induced convection of solution takes a key role in the observed MFEs.

Conclusions

Using a biased random walk simulation, the DLA patterns of copper and silver dendrites in a magnetic field gradient are evaluated. The effect of a high magnetic field gradient can be simulated by simply varying the drift probabilities of the particles which is induced by a magnetic force. Not only the patterns but also the chemical yields of copper and silver dendrites are reproduced by the simulation. It is confirmed, from computer simulation, that a magnetic force produced by a high magnetic field gradient induces convection of solution. This affects the deposition patterns and yields of copper and silver dendrites.

Authors acknowledge the reviewers for valuable suggestions and comments. This work was supported in part by the Grant-in-Aid for Scientific Research from the Ministry of Education, Science, Sports and Culture and in part by Iwatani Naoji Foundation's Research Grant.

References

1 For example, see: a) Y. Tanimoto, "Functionality of Molecular Systems 1", ed by S. Nagakura, Springer-Verlag, Tokyo (1998), p. 301. b) S. Nagakura, H. Hayashi, and T. Azumi (eds), "Dynamic Spin Chemistry," Kodansha/Wiley, Tokyo (1998), Chaps. 2—5. c) Abstract of International Workshop on Chemical, Physical and Biological Processes under High Magnetic Field, Omiya, November 1999.

2 a) M. Mukai, Y. Fujiwara, Y. Tanimoto, and M. Okazaki, *J. Phys. Chem.*, **97**, 12660 (1993). b) Y. Fujiwara, T. Aoki, K. Yoda, H. Cao, M. Mukai, T. Haino, Y. Fukazawa, Y. Tanimoto, H. Yonemura, T. Matsuo, and M. Okazaki, *Chem. Phys. Lett.*, **259**, 361 (1996). c) H. Cao, K. Miyata, T. Tamura, Y. Fujiwara, A. Katsuki, C.-H. Tung, and Y. Tanimoto, *J. Phys. Chem. A*, **101**, 407 (1997). d) R. Nakagaki, M. Yamaoka, O. Takahira, K. Hiruta, Y. Fujiwara, and Y. Tanimoto, *J. Phys. Chem. A*, **101**, 556 (1997). e) Y. Fujiwara, T. Aoki, T. Haino, Y. Fukazawa, Y. Tanimoto, R. Nakagaki, O. Takahira, and M. Okazaki, *J. Phys. Chem. A*, **101**, 6842 (1997). f) Y. Tanimoto, H. Tanaka, Y. Fujiwara, and M. Fujiwara, *J. Phys. Chem. A*, **102**, 5611 (1998). g) Y. Fujiwara, K. Yoda, T. Tomonari, T. Aoki, Y. Akimoto, and Y. Tanimoto, *Bull. Chem. Soc. Jpn.*, **72**, 1705 (1999). h) R. De, Y. Fujiwara, T. Haino, and Y. Tanimoto, *Chem. Phys. Lett.*, **315**, 383 (1999).

3 a) A. Katsuki, S. Watanabe, R. Tokunaga, and Y. Tanimoto, *Chem. Lett.*, **1996**, 219. b) Y. Tanimoto, A. Katsuki, H. Yano, and S. Watanabe, *J. Phys. Chem. A*, **101**, 7359 (1997). c) W. Duan, H. Yano, and Y. Tanimoto, *Fractals*, **6**, 145 (1998). d) Y. Tanimoto, H. Yano, S. Watanabe, A. Katsuki, W. Duan, and M. Fujiwara, *Bull. Chem. Soc. Jpn.*, **73**, 867 (2000).

4 a) A. Katsuki, R. Tokunaga, S. Watanabe, and Y. Tanimoto, *Chem. Lett.*, **1996**, 607 (1996). b) M. Fujiwara, T. Chidiwa, R. Tokunaga, and Y. Tanimoto, *J. Phys. Chem. B*, **102**, 3417 (1998). c) M. Fujiwara, R. Tokunaga, and Y. Tanimoto, *J. Phys. Chem. B*, **102**, 5996 (1998). d) M. Fujiwara, M. Fukui, and Y. Tanimoto, *J. Phys. Chem. B*, **103**, 2627 (1999).

5 Y. Tanimoto, S. Izumi, K. Furuta, T. Suzuki, Y. Fujiwara, T. Hirata, G. Yamada, and K. Itoh, *Environ. Sci.*, **13**, 61 (2000).

6 a) I. Mogi, S. Okubo, and Y. Nakagawa, *J. Phys. Soc. Jpn.*, **60**, 3200 (1991). b) S. Okubo, I. Mogi, and Y. Nakagawa, "Pattern Formation in Complex Dissipative Systems," ed by S. Kai, World Science, Singapore (1992), P. 98. c) I. Mogi, S. Okubo, and Y. Nakagawa, *J. Cryst. Growth*, **128**, 258 (1993). d) S. Okubo, I. Mogi, G. Kido, and Y. Nakagawa, *Fractals*, **1**, 425 (1993). e) I. Mogi, M. Kamiko, and S. Okubo, *Fractals*, **1**, 475 (1993). f) I. Mogi and S. Okubo, *Physica. B*, **211**, 319 (1995). g) I. Mogi, *Fractals*, **3**, 371 (1995).

7 a) T. A. Witten and L. M. Sander, *Phys. Rev. Lett.*, **47**, 1400 (1981). b) T. A. Witten and L. M. Sander, *Phys. Rev. B*, **27**, 5686 (1983).

8 a) Meakin, *Phys. Rev. A*, **27**, 1495 (1983). b) Meakin, *Phys. Rev. B*, **28**, 5221 (1983). c) Meakin and J. M. Deutch, *J. Chem. Phys.*, **80**, 2115 (1984).

9 a) Y. Sawada, S. Ohta, M. Yamazaki, and H. Honjo, *Phys. Rev. A*, **26**, 3557 (1982). b) Y. Sawada, A. Doughtly, and J. P. Gollub, *Phys. Rev. Lett.*, **56**, 1260 (1986).

10 a) T. Nagatani and F. Sagues, *J. Phys. Soc. Jpn.*, **59**, 3447 (1990). b) T. Nagatani and F. Sagues, *Phys. Rev. A*, **43**, 2970 (1991).

11 a) R. F. Voss, *Phys. Rev. B*, **30**, 334 (1984). b) R. F. Voss and M. Tomkievicz, *J. Electrochem. Soc.*, **132**, 371 (1985).